Cell Cycle 10:15, 2592-2602; August 1, 2011; © 2011 Landes Bioscience

Siah1/SIP regulates p27^{kip1} stability and cell migration under metabolic stress

Yoshito Nagano,[1,†] Toru Fukushima,[1,†,‡] Kazuo Okemoto,[1] Keiichiro Tanaka,[1] David D.L. Bowtell,[2,3] Ze'ev A. Ronai,[1] John C. Reed[1] and Shu-ichi Matsuzawa[1,*]

[1]Sanford-Burnham Medical Research Institute; La Jolla, CA USA; [2]Peter MacCallum Cancer Centre; Department of Research; Cancer Genomics and Biochemistry Laboratory; [3]University of Melbourne; Department of Biochemistry and Molecular Biology; Melbourne, VIC Australia

[‡]Current address: Department of Diabetes and Clinical Nutrition; Graduate School of Medicine; Kyoto University; Kyoto, Japan

[†]These authors contributed equally to this work.

Key words: p27^{kip1}, Siah1, SIP, glucose starvation, cell migration

p27^{kip1} has been implicated in cell cycle regulation, functioning as an inhibitor of cyclin-dependent kinase activity. In addition, p27 was also shown to affect cell migration, with accumulation of cytoplasmic p27 associated with tumor invasiveness. However, the mechanism underlying p27 regulation as a cytoplasmic protein is poorly understood. Here we show that glucose starvation induces proteasome-dependent degradation of cytoplasmic p27, accompanied by a decrease in cell motility. We also show that the glucose limitation-induced p27 degradation is regulated through an ubiquitin E3 ligase complex involving Siah1 and SIP/CacyBP. *SIP*$^{-/-}$ embryonic fibroblasts have increased levels of cytosolic p27 and exhibit increased cell motility compared with wild-type cells. These observations suggest that the Siah1/SIP E3 ligase complex regulates cell motility through degradation of p27.

Introduction

Through its nuclear localization, p27^{kip1} is an important cell cycle regulator, whose principal role in cell cycle is to inhibit cyclin-dependent kinases.[1-5] Recently, p27 was also shown to reside in the cytosol, where it contributes to cell migration.[6,7] These observations suggest that, depending on its subcellular localization, p27 can have dual functions with implications for tumor development and tumor suppression. Indeed, *p27*-null mice develop multi-organ hyperplasia and have increased susceptibility to cancer.[8-10] Reduced levels of nuclear p27 protein have been associated with poor prognosis in many types of human cancers.[11,12] Translocation of p27 protein to the cytoplasm is associated with poor patient prognosis in breast tumor malignancies.[13-15] Moreover, accumulation of cytoplasmic p27 protein has also been reported in other human malignancies.[16,17]

The gene encoding p27 is rarely mutated in tumor cells that express low levels of the protein, suggesting an important role for post-transcriptional mechanisms in p27 turnover. Indeed, nuclear p27 is degraded by the SCF^{Skp2} complex during late G_1 phase.[18-21] In this context, the F-box protein Skp2 acts as an adaptor that recognizes p27 phosphorylated at threonine residue 187 (T187), which facilitates its ubiquitination.[22] However, analysis of a T187A knock-in mouse model showed that while mutated p27 was stabilized in S phase, it was still degraded normally during G_0 and G_1 phase suggesting that other proteolytic degradation pathways exist.[23] In fact, another E3 ligase complex containing KPC1 and KPC2 was identified that induces the degradation of cytoplasmic p27 during the G_1 phase.[24] These degradation pathways are activated during cell cycle progression. Recently, it has been suggested that another p27 turnover pathway acts in the nucleus during cell cycle transition from the G_0 to G_1 phase.[25] Moreover, phosphorylation at T198 controls p27 stability during G_0 to G_1 transition, however, the E3 ligase that regulates this pathway remains unknown.

Siah/Sina-family proteins represent mammalian homologs of the Drosophila Sina (seven in absentia) protein[26-28] and are E3 ubiquitin ligases that regulate ubiquitination and protein degradation.[29] In certain cases, Siah-mediated degradation requires the presence of adaptor proteins, such as the Siah Interacting Protein (SIP/CacyBP).[30-34] Previously we discovered a novel pathway for p53-induced β-Catenin degradation that involves a series of protein interactions between E3 ligase Siah1, SIP, Skp1 and Ebi, a F-box protein that binds β-Catenin.[30] Siah1 expression is induced by p53,[28,35-38] thereby linking genotoxic injury to destruction of β-Catenin, reducing the activity of β-Catenin-binding Tcf/LEF transcription factors, and eventually contributing to cell cycle arrest.[30]

To gain insights into the physiological relevance of this degradation pathway in vivo, we recently generated knockout mice lacking SIP.[39] In addition to the expected increase in β-Catenin expression, *SIP*$^{-/-}$ embryonic fibroblasts exhibited increased levels

*Correspondence to: Shu-ichi Matsuzawa; Email: smatsuzawa@sanfordburnham.org
Submitted: 06/12/11; Accepted: 06/13/11
DOI: 10.4161/cc.10.15.16912

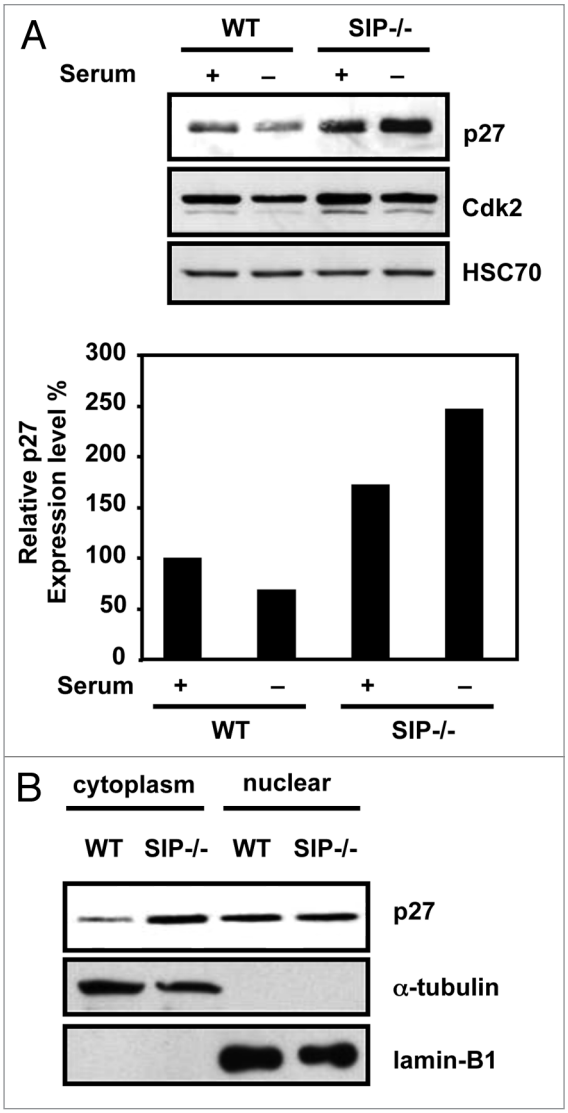

Figure 1. Cytoplasmic p27 accumulates in SIP-deficient MEFs. (A) (Top) Wild-type and *SIP*$^{-/-}$ MEFs were cultured in media containing 10% FCS (+) or 0.1% FCS (-) for 24 h. Cell lysates were analyzed by immunoblotting using antibodies specific for p27, Cdk2 or Hsc70. Representative experiment is shown. (Bottom) The degree of p27 expression was quantified by densitometric analysis with ImageJ software and expressed as a percentage of p27 expression in wild-type MEFs under normal growth conditions. Data are average of three time experiments. (B) Wild-type and *SIP*$^{-/-}$ MEFs cultured in complete media. Cell lysates were fractionated and analyzed by immunoblotting using antibodies specific for p27, Lamin B1 and α-tubulin, which acted as markers for the cytoplasmic and nuclear fractions, respectively.

of cytoplasmic p27. We found that cytoplasmic p27 is degraded after glucose starvation independent of cell cycle. Glucose limitation-induced p27 degradation is limited to cytoplasmic p27 and is Siah1/SIP-dependent. Correspondingly, *SIP*$^{-/-}$ embryonic fibroblasts exhibit an increased cell motility compared with wild-type cells, consistent with the reported role of p27 in cell motility. These observations suggest that glucose levels regulate cytosolic p27 availability, with concomitant impact on cell motility, via the SIP/Siah ubiquitin ligase complex.

Results

Accumulation of p27 protein in the cytoplasm of SIP-deficient cells. In the course of analyzing *SIP*$^{-/-}$ mice, we observed that p27 protein levels were elevated approximately 1.7-fold in proliferative and 3.6-fold in non-proliferative *SIP*$^{-/-}$ mouse embryonic fibroblasts (MEFs) compared with wild-type MEFs (**Fig. 1A**). In contrast, levels of other cell cycle regulators, such as p21$^{waf1/cip1}$, Cyclin A, Cyclin D1, Cyclin E, Cdk2 and Cdk4 did not change (data not shown). Because p27 has multiple functions depending on its subcellular localization, we next fractionated cell lysates to obtain nuclear and cytoplasmic fractions and examined levels of p27. Elevated p27 protein levels were observed in the cytoplasmic but not the nuclear fraction of *SIP*$^{-/-}$ cells (**Fig. 1B**). These results suggest that SIP deficiency is involved in cytoplasmic p27 accumulation.

Glucose limitation induces p27 degradation. Recently, it has been reported that stability of p27 is controlled by metabolic stress.[25] To examine whether p27 is degraded by various metabolic stress, NIH3T3 cells were cultured in nutrient-poor conditions, such as serum deprivation, starved of glucose or subjected to amino acid deprivation and the levels of endogenous p27 examined. As shown in **Figure 2A**, glucose limitation triggered a striking decrease in p27 levels in NIH3T3 cells, which is in contrast to the steady p27 levels observed under conditions of serum-starvation or amino acid-deprivation (**Fig. 2A**). Levels of other cell cycle regulators, such as p21, Cyclin A, Cyclin D1, Cyclin E, Cdk2 and Cdk4, did not change (data not shown).

In light of these findings, we explored the effect of glucose limitation on p27 stability in greater detail. For these experiments, MEFs were prepared from wild-type mouse embryos and cultured in media containing 0.1% FBS for 48 h to synchronize the cell cycle. These synchronized cells were then subjected to glucose-starvation in the presence of 10% FBS and the levels of endogenous p27 protein were monitored by immunoblotting. Under normal growth conditions, the p27 protein level gradually decreased up to 30 h after serum addition but recovered by 36 h (**Fig. 2B**), consistent with previous reports showing that p27 is degraded by the KPC1/2 [24] and the SCF^{Skp2} complex during the G_1 phase.[18-20] In contrast, low glucose (0.1 mM) triggered a rapid decline in endogenous p27 protein levels after 3 h and the levels did not recover (**Fig. 2B**). Under glucose-deprived conditions, these cells were able to progress through the cell cycle in the presence of 10% FBS (**Fig. 2C**).

We next examined the effects of SIP deficiency on p27 stability in response to glucose limitation. As shown in **Figure 2B**, glucose limitation triggered a decrease in endogenous p27 protein levels in MEFs from wild-type *SIP*$^{+/+}$ and heterozygous *SIP*$^{+/-}$ mice (data not shown). In contrast, p27 levels in homozygous *SIP*$^{-/-}$ MEFs were recovered after 24 h. These observations suggest that SIP is involved in the pathway for the glucose limitation-induced degradation of p27 proteins.

Glucose limitation induces poly-ubiquitination of cytoplasmic p27 proteins. Because SIP has been implicated in the regulation of protein stability via the E3 ubiquitin ligase Siah1, we assessed SIP-dependent changes in p27 ubiquitination. To this

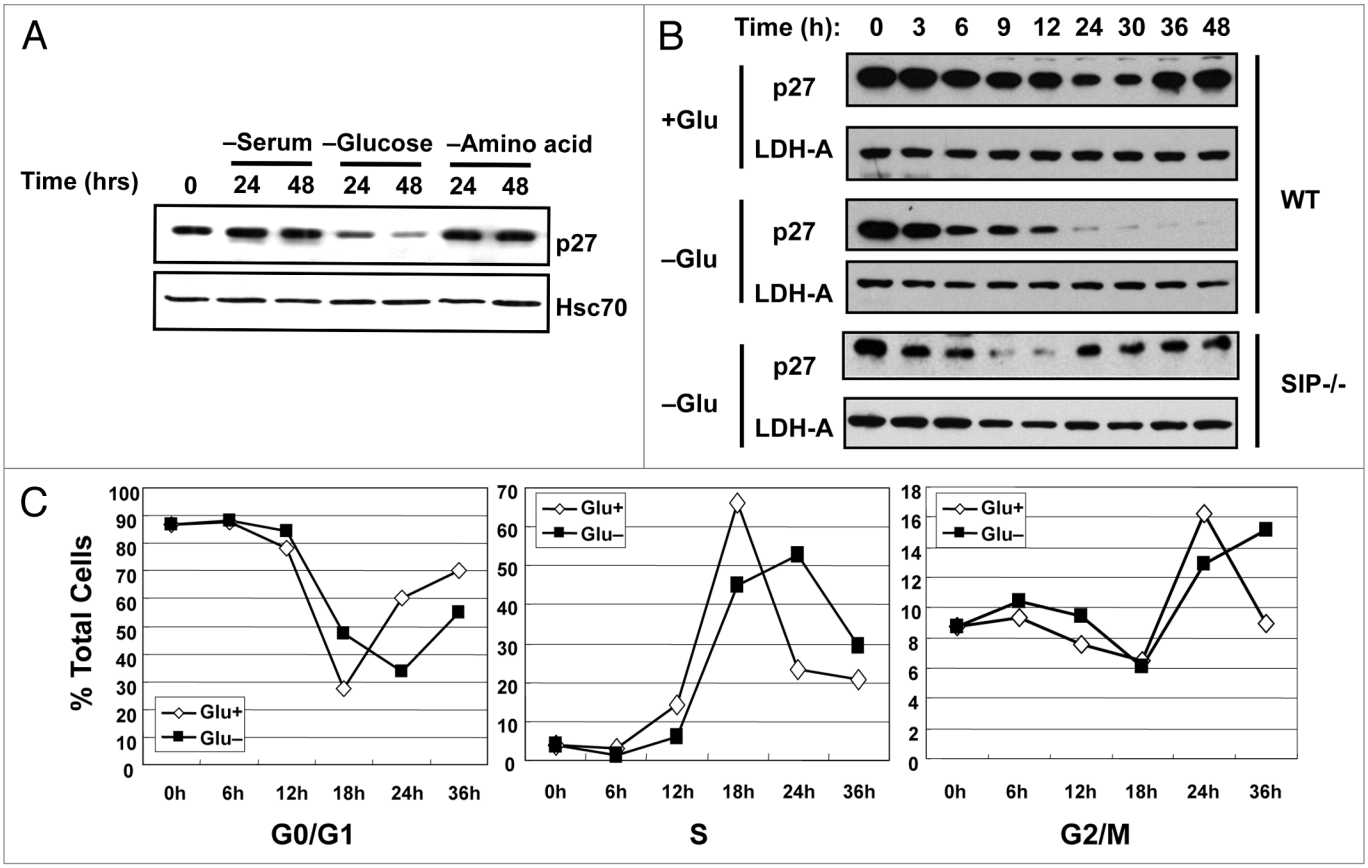

Figure 2. Glucose starvation induces degradation of p27. (A) NIH3T3 cells were cultured in low (0.1% FCS) or normal (10% FCS) serum in the presence of absence of glucose or amino acids for the indicated times. Whole cell lysates were analyzed by immunoblotting using antibodies specific for p27 and Hsc70 to confirm consistent protein loading. (B) Wild-type (WT) and *SIP*$^{-/-}$ (SIP$^{-/-}$) MEFs were synchronized by serum starvation for 48 h and the cells cultured in media containing 0.1 mM glucose (-Glu) or 25 mM glucose (+Glu) for the indicated times. Whole cell lysates were prepared and subjected to immunoblotting using anti-p27 and anti-LDH-A as a control. (C) Cell cycle analysis after glucose limitation. Serum-starved MEFs were released into complete media or glucose free media. Cells were treated with BrdU (20 μM) for 20 min prior to cell harvest. At the indicated times, cells were harvested and analyzed by flow cytometry. The percentage of cells in each phase of the cell cycle is shown in each graph.

end, p27 was immunoprecipitated from glucose-deprived *SIP*$^{+/+}$ and *SIP*$^{-/-}$ MEFs in the presence of MG132 and assessed for the degree of ubiquitination. Significantly, glucose limitation triggered poly-ubiquitination of p27 protein in *SIP*$^{+/+}$ mice but not in *SIP*$^{-/-}$ MEFs (**Fig. 3A**).

The effect of glucose limitation on p27 protein stability was further examined by cycloheximide chase experiments. *SIP*$^{+/+}$ and *SIP*$^{-/-}$ MEFs transfected with Myc-tagged p27, were cultured in low glucose media for 48 h. Then, cells were treated with 25 μg/ml cycloheximide and the rate of p27 turnover was monitored. In *SIP*$^{+/+}$ MEFs, a half-life of several hours was seen for Myc-p27 (**Fig. 3B**). In contrast, Myc-p27 protein was significantly more stable in *SIP*$^{-/-}$ MEFs, compared with *SIP*$^{+/+}$ MEFs. These results demonstrate that glucose limitation downregulates p27 in a post-translational manner and that SIP deficiency stabilizes p27.

To investigate whether the glucose limitation-induced degradation of p27 occurs in the cytoplasm, wild-type and *SIP*$^{-/-}$ MEFs were subjected to glucose starvation, and the levels of endogenous p27 protein were examined in cytosolic vs. nuclear fractions. Downregulation of p27 levels in the nuclear fraction, which is regulated by Skp2, was observed in both *SIP*$^{+/+}$ and *SIP*$^{-/-}$ MEFs (**Fig. 3C**). In contrast, downregulation of p27 in the cytosolic fraction was observed in *SIP*$^{+/+}$ MEFs but not in *SIP*$^{-/-}$ MEFs suggesting that the degradation of p27 in cytoplasm is SIP-dependent. A p27 mutant (p27ΔNLS) [24] that localizes exclusively to the cytosol was also degraded by glucose-starvation, supporting the hypothesis that glucose limitation-induced degradation of p27 occurs mainly in the cytoplasm (**Fig. 3D**).

Siah1 is required for glucose limitation-induced p27 degradation. Since SIP's effect on protein ubiquitination and stability must be mediated through an associated ubiquitin ligase, and since Siah is among SIP-bound ligases, we directly assessed the role of Siah on p27 stability. To investigate whether Siah1/SIP contributes to the degradation of p27 in vivo, we examined the potential interaction of p27 and the Siah1/SIP complex by co-immunoprecipitation experiments. An expression plasmid encoding HA epitope-tagged p27 was transfected into HEK293T cells either alone or in combination with plasmids encoding FLAG-epitope-tagged Siah1 and Myc-tagged SIP. The resulting cell lysates were immunoprecipitated using a monoclonal antibody specific for the HA epitope with associated FLAG-Siah1 and Myc-SIP detected by immunoblotting using an anti-FLAG or anti-Myc

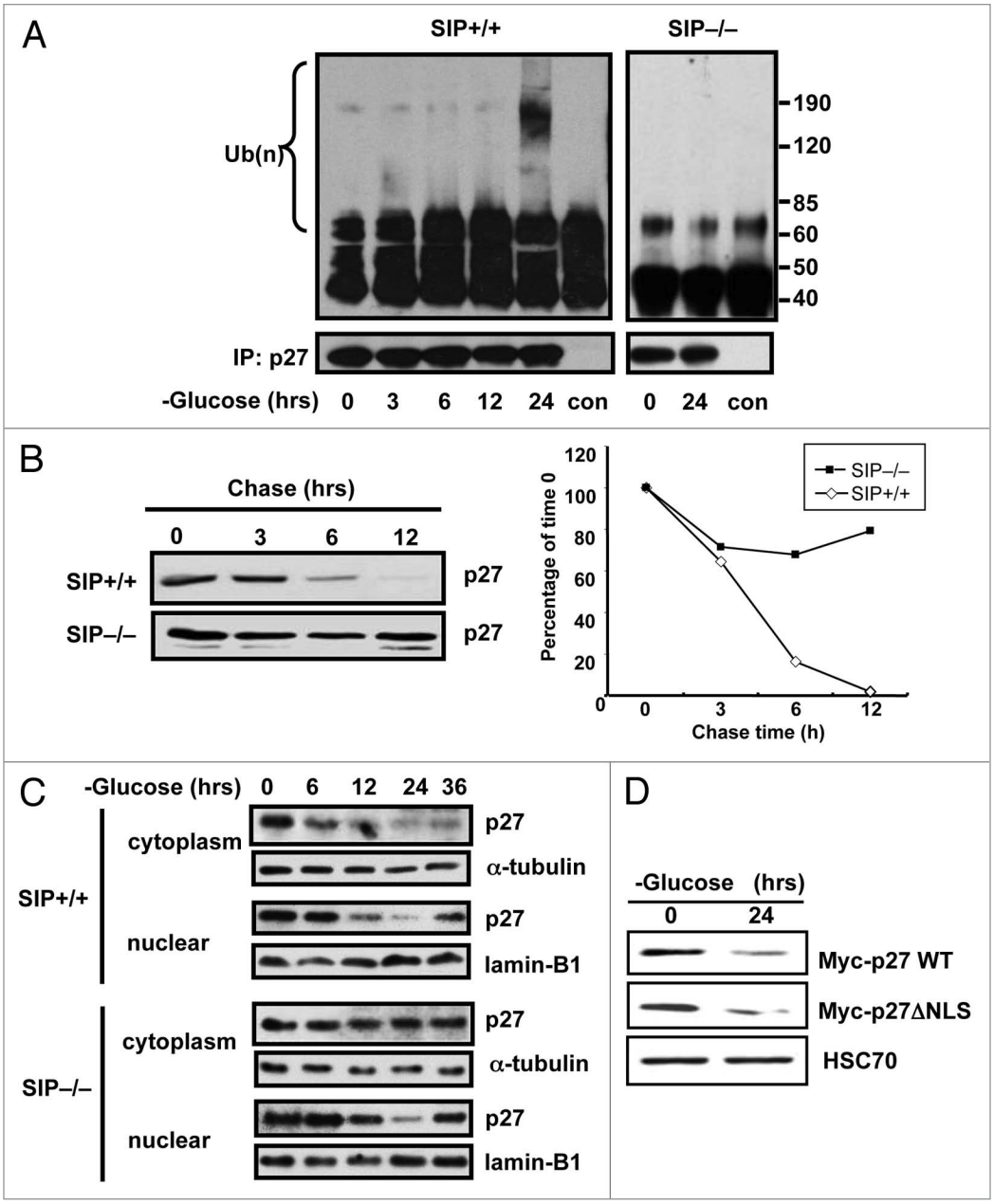

Figure 3. Glucose limitation induces poly-ubiquitination of cytoplasmic p27 protein. (A) Synchronized wild-type and *SIP*$^{-/-}$ MEFs were cultured in low glucose media and 10% dialyzed FCS and cell lysates prepared at the indicated times. Endogenous p27 proteins were immunoprecipitated with anti-p27 antibody and the immunoprecipitates analyzed by immunoblotting with anti-ubiquitin or p27 antibodies. (B) Wild-type or *SIP*$^{-/-}$ MEFs cells in 100 mm dishes were transiently transfected with 3 μg of plasmids producing with Myc-tagged p27 plasmid for 48 h and cells were cultured in glucose free media. After 48 h, cells were treated with 25 μg/ml cycloheximide, were harvested at the indicated times and an equal amount of protein from each lysate was analyzed by immunoblotting using anti-Myc antibody. The degree of p27 expression was quantitated by densitometric analysis with ImageJ software and expressed as a percentage of p27 expression at 0 h. (C) Synchronized wild-type and *SIP*$^{-/-}$ MEFs were cultured in low glucose media and cell lysates were prepared at the indicated times. Cell lysates were fractionated to cytosolic and nuclear fractions and levels of p27 proteins analyzed by immunoblotting using anti-p27, Lamin B1 and α-tubulin antibodies. (D) NIH3T3 cells stably expressing Myc-tagged wild-type p27 or mutant of nuclear localization signal p27 (ΔNLS) were cultured in media containing 0.1 mM glucose and 10% dialyzed FCS. After 48 h, cell lysates were analyzed by immunoblotting using antibodies specific for Myc and HSC70.

monoclonal antibody. As shown in **Figure 4A**, both FLAG-Siah1 and Myc-SIP were co-immunoprecipitated with HA-p27. Expression of all proteins was confirmed by immunoblot analysis of lysates generated from the transfected HEK293T cells. A physiological interaction between endogenous Siah1 and endogenous p27 protein was also demonstrated by co-immunoprecipitation using anti-p27 antibody followed by immunoblot analysis using anti-Siah1 antibodies (**Fig. 4B**). The interaction between Siah1 and p27 in the cytoplasm was maximal at ~24 h after glucose limitation, which is consistent with p27 poly-ubiquitination. In

contrast, the interaction between Siah1 and p27 was not observed in nuclear fractions.

The kinetics and dose-dependency of p27 degradation were examined (**Fig. 5A**). Downregulation of endogenous p27 protein levels occurs at glucose concentrations below 1 mM. Interestingly, Siah1 expression increased in the presence of ≤1 mM glucose—the same conditions under which p27 degradation is observed (**Fig. 5A**). Time-course experiments showed a clear correlation between p27 degradation and induction of Siah1 expression (**Fig. 5B**). To determine whether Siah1 is required for the glucose limitation-induced degradation of p27, NIH3T3 cells were transiently transfected with plasmids encoding HA-tagged Phyllopod peptide (phyl-pep) which outcompetes adaptor proteins required for Siah association with some of its substrates,[40] or RING mutant forms of Siah, Siah1ΔR and Siah2ΔR, that exhibit a dominant-negative effect on endogenous Siah1 and Siah2, respectively. Glucose-starvation of NIH3T3 cells expressing the inhibitors of Siah was followed by analysis of endogenous p27 protein levels. As shown in **Figure 5C**, expression of either phyl-pep or dominant-negative Siah proteins attenuated the effects of glucose limitation on p27 degradation, suggesting that Siah proteins contribute to the degradation.

The effect of Siah1 on p27 degradation was also confirmed by overexpression assays. Accordingly, HEK293T cells were transiently transfected with plasmids encoding HA-tagged p27 alone or in combination with plasmids producing Siah1 and dominant-negative Siah1 (Siah1ΔR). The steady-state levels of transgene-derived p27 were then monitored by immunoblotting. Overexpression of Siah1 resulted in a marked (>90%) decrease in p27 protein levels (**Fig. 5D**). Moreover, addition of a proteasome inhibitor (MG132) to the culture medium prevented Siah1-induced degradation of p27 (**Fig. 5D**), confirming a proteasome-dependent degradation process. In contrast to Siah1, expression of the Siah1ΔR protein in HEK293T cells did not decrease levels of HA-p27 protein, consistent with the inability of this protein to bind Ubiquitin-conjugating enzymes (Ubcs). We conclude therefore that Siah1 promotes the degradation of p27.

Because we previously demonstrated a sequence of protein interactions leading to Siah1-induced β-Catenin degradation:

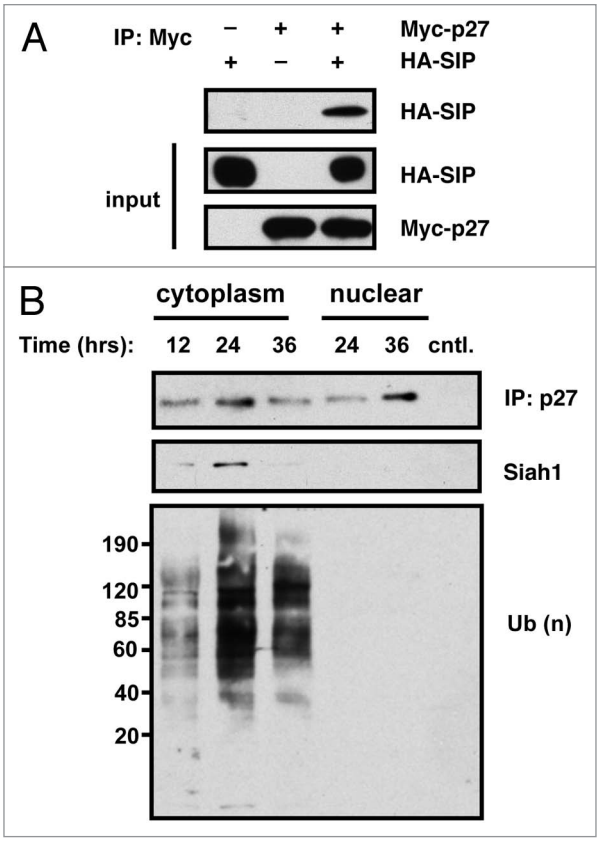

Figure 4. p27 associates with Siah1/SIP in cells. (A) HEK293T cells in 100 mm dishes were transfected with 3 μg each of plasmids producing Myc-tagged p27 and HA-tagged SIP (total DNA = 6 μg). Controls (-) represent cells transfected with HA or Myc-tagged pcDNA3 lacking a cDNA insert. Lysates were prepared and either loaded directly in gels (25 μg total protein content) (labeled as "input") or used for immunoprecipitations employing anti-Myc antibody. Immune-complexes were analyzed by SDS-PAGE/immunoblotting using anti-HA and Myc antibodies with ECL-based detection. (B) Synchronized wild-type MEFs were cultured in low glucose media and 10% dialyzed FCS and the cytosolic fraction prepared from cell lysates at the indicated times. Endogenous p27 proteins were immunoprecipitated with anti-p27 antibody and immunoprecipitates were analyzed by immunoblotting with anti-Siah1, ubiquitin or p27 antibodies.

Figure 5 (See opposite page). Siah1 is required for glucose limitation-induced p27 degradation. (A) Wild-type MEFs were cultured in media containing 10% dialyzed FCS and various concentrations of glucose. After 2 d, cell lysates were analyzed by immunoblotting using anti p27 or Siah1 antibodies. The membrane was reprobed with anti-HSC70 antibody as a control. (B) Wild-type MEFs cultured in complete media were released into glucose-free media. At the indicated times, lysates were analyzed by immunoblotting using antibodies for p27, Siah1 or LDH-A. (C) NIH3T3 cells were transiently transfected with plasmids encoding HA-Phyllopod or FLAG-Siah1ΔR and FLAG-Siah2ΔR as indicated. After 24 h, cell lysates were prepared from duplicate dishes for each transfection and analyzed by SDS-PAGE/immunoblotting using antibodies specific for p27, HA, FLAG and Hsc70 with ECL-based detection. (D) HEK293T cells were transiently transfected with plasmids encoding HA-p27, FLAG-Siah1 or FLAG-Siah1ΔR in various combinations as indicated (total DNA amount normalized). After 24 h, cell lysates were prepared from duplicate dishes of each transfection and analyzed by SDS-PAGE/immunoblotting using antibodies specific for HA and FLAG, with ECL-based detection. (E) HEK293T cells were transiently transfected with plasmids encoding HA-p27 (0.5 μg), FLAG-Siah1 (0.5 μg), Myc-SIP (0.5 μg), Myc-SIP-S (0.5 μg) or Myc-Skp2ΔF (0.5 μg) in various combinations as indicated (total DNA amount normalized). After 24 h, cell lysates were prepared from duplicate dishes of each transfection, normalized for total protein content (20 μg per lane) and analyzed by SDS-PAGE/immunoblotting using antibodies specific for HA-tag, FLAG or Myc, with ECL-based detection. (F) NIH3T3 cells were transiently transfected with plasmids encoding Myc-p27, FLAG-Siah1 and HA-SIP in various combinations as indicated (total DNA amount normalized). After 24 h, cells were treated with 1 μM MG132 for 6 h. Lysates were immunoprecipitated with anti-Myc antibody. Immunoprecipitates were divided into two partss and analyzed immunoblotting using anti-ubiquitin and anti-Myc antibodies. Expression of Myc-p27, HA-SIP in each total cell lysate was detected with anti-ubiquitin, -Myc, -HA and -FLAG antibodies. (G) Synchronized wild-type and *Siah1a*$^{-/-}$ MEFs were cultured in media containing 0.1 mM glucose and 10% dialyzed FCS. Cell lysates were prepared at the indicated times and subjected to immunoblotting with anti-p27 and LDH-A antibodies.

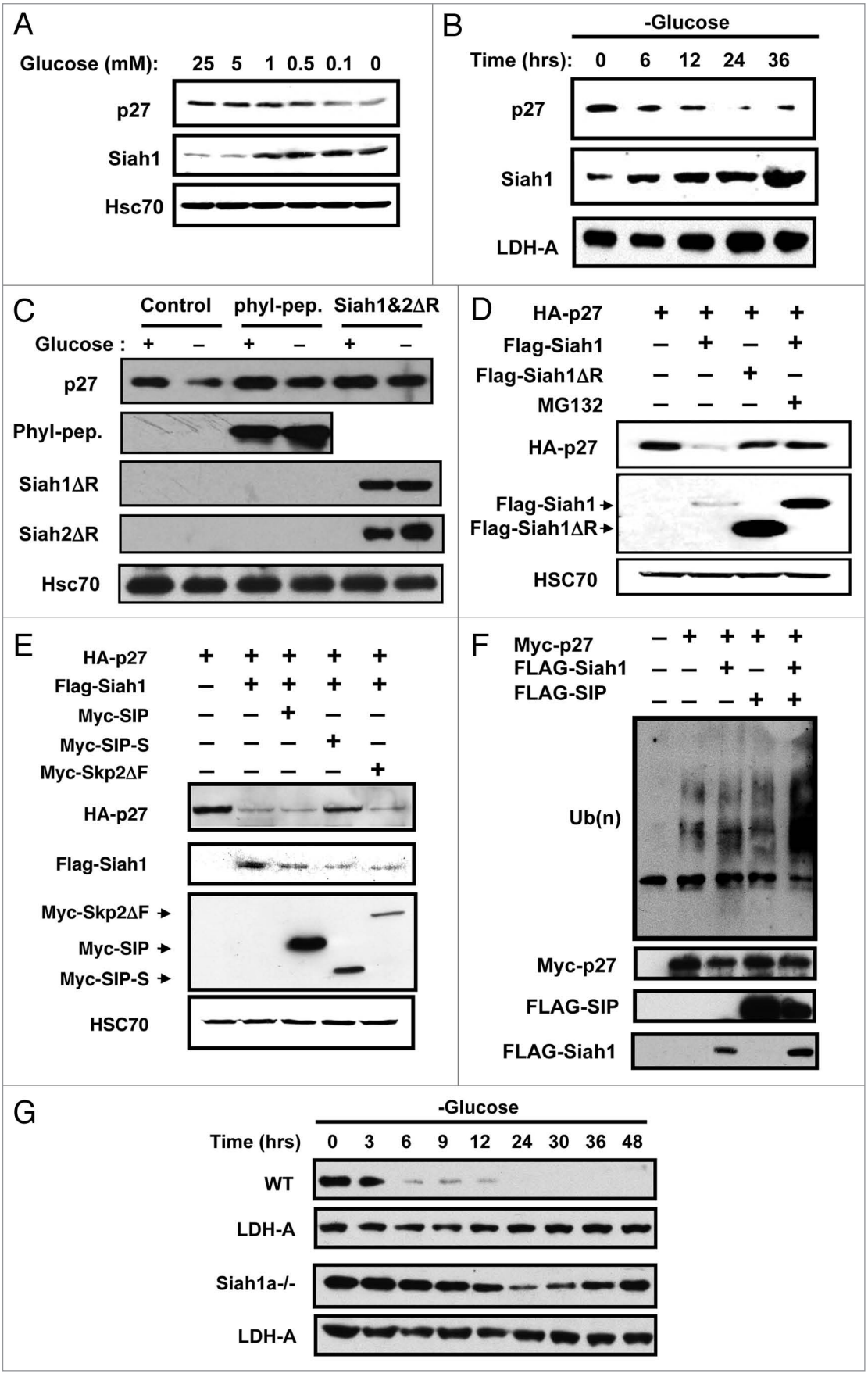

Figure 5. For figure legend see page 2596.

Siah1→SIP→Skp1→Ebi→β-Catenin, we explored the roles of SIP and Ebi in the mechanism by which Siah1 induces p27 degradation. Co-expressing dominant-negative SIP-S, which cannot bind to Siah1,[30] blocked/attenuated the effects of Siah1 on p27 degradation, restoring p27 to control levels (**Fig. 5E**). In contrast, dominant-negative Ebi lacking the F-box doman (EbiΔF) [30] failed to interfere with Siah1-induced p27 degradation (data not shown). Co-expression of dominant-negative Skp2 protein (Skp2ΔF), another F-box protein that recognizes phosphorylated p27 on Thr187 and facilitates its ubiquitination in the late G_1 and S phase, also did not interfere with Siah1-induced p27 degradation. Correspondingly, co-expression of Siah1 and SIP induced poly-ubiquitination of p27 in NIH3T3 cells (**Fig. 5F**). We deduce from these experiments that Siah1-induced degradation of p27 is SIP-dependent, but Ebi- or Skp2-independent.

We next examined the effects of Siah1 deficiency on p27 stability in response to glucose limitation (**Fig. 5G**). For these experiments, early passage MEFs were prepared from *Siah1a*$^{-/-}$ embryos, subjected to glucose-starvation, and the levels of endogenous p27 protein were evaluated by immunoblotting. Homozygous *Siah1a*$^{-/-}$ MEFs failed to downregulate p27, suggesting that Siah1 is necessary for the glucose limitation-induced degradation of p27 protein (**Fig. 5G**).

Increased migration of cells lacking SIP. In addition to its role in cell cycle control, p27 was recently shown to affect cell migration by regulating Rho proteins.[7,41,42] Notably, these distinct functions are associated with nuclear or cytosolic localization of p27, respectively. Moreover, accumulation of cytoplasmic p27 protein has been recognized to be associated with tumor malignancies, suggesting a role in tumor invasion.[16,17,43,44] Therefore, we explored the effect of SIP on cell motility. Initially, cell migration was monitored using transwell chambers that were seeded with MEFs derived from wild-type or *SIP*$^{-/-}$ embryos using low or high serum that was supplemented (or not) with glucose. *SIP*$^{+/+}$ and *SIP*$^{-/-}$ MEFs displayed comparable motility when cultured with glucose, though *SIP*$^{-/-}$ MEFs exhibited slightly greater motility (**Fig. 6A**). Significantly, under glucose-depleted conditions, wild-type MEFs exhibited a marked reduction in migration, while *SIP*$^{-/-}$ MEFs showed significantly enhanced migration. Serine 10 phosphorylation of p27 correlates with increased stability and cytoplasmic export.[45,46] Moreover, NIH3T3 cells expressing mutant of S10 phospho-mimetic residue p27 (S10D) or p27 (ΔNLS) also showed significantly enhanced migration (**Fig. 6A**).

The effect of SIP deficiency on glucose-dependent cell migration was confirmed using an independent assay, namely an in vitro "wound healing" model wherein cell monolayers are scrapped and the migration of cells into the denuded region of the plastic culture dish is monitored over time (**Fig. 6B**). Consistent with the motility assay findings, striking differences in cell migration were observed in the wound healing model when *SIP*$^{+/+}$ and *SIP*$^{-/-}$ MEFs were cultured in glucose-deprived medium, with SIP-deficient MEFs filling the denuded area faster. These results corroborate the findings obtained by the transwell method. Overall, the data indicate that inhibition of migration in response to glucose limitation is impaired in *SIP*$^{-/-}$ MEFs, showing that glucose-dependent cell migration is regulated by SIP.

Discussion

In this study, we show that glucose limitation induces Siah/SIP-dependent degradation of the cytoplasmic p27 protein. p27 is a well known inhibitor of cell proliferation. However, recent studies show that p27 has an alternative function, acting in the cytoplasm to regulate Rho signaling and thereby controlling cytoskeletal organization and cell motility.[47] In this regard, p27 binds to RhoA and prevents the interaction of RhoA with guanine-nucleotide exchange factors. RhoA promotes the formation of actin stress fibers and focal adhesions through the recruitment and activation of its effectors mammalian diaphanous (mDIA) and the Rho kinases ROCK1/2.[47] We also show that *SIP*$^{-/-}$ embryonic fibroblasts are deficient in their ability to downregulate p27 levels and display faster cell migration rates. Furthermore, a recent study has shown that downregulation of SIP by RNA interference increases tumorigenicity and invasiveness of gastric cancer cells.[48] Recently, Schneider and coworkers reported that SIP interacts with tubulin to increase tubulin assemblies in neuroblastoma cells, suggesting that SIP/CacyBP regulates microtubule dynamics and plays a role in cell migration.[49] Thus, we hypothesize that via their degradation of cytosolic p27, Siah/SIP plays important roles in cell motility.

Genotoxic stress triggers the activation of kinases that phosphorylate and activate tumor suppressor p53, arresting cells in G_1 phase to prevent replication of damaged DNA. In addition to DNA damage, limitation of nutrients, such as glucose or amino acids, is known to induce cell cycle arrest via p53-dependent mechanisms. For example, cells exposed to low glucose and low serum arrest in the G_1 phase of the cell cycle,[50] regulated by AMP-activated protein kinase (AMPK), which in turn is activated by LKB1.[51] AMPK activation induces p53 phosphorylation, which is essential for promoting p53-dependent cell cycle arrest.[50] In our study, we observed Siah1 expression and p27 degradation induced by glucose limitation when cells were supplemented with 10% serum. In the presence of serum, cells progressed through the cell cycle normally and increased levels of senescence were not observed (**Fig. S1A**). However, when MEFs were treated with low glucose and low serum, then more than 60% of MEFs underwent senescence, although p27 was not downregulated under such conditions (**Fig. S1B**). Although *SIP*$^{-/-}$ and *Siah1a*$^{-/-}$ MEFs failed to degrade p27, these cells are not impaired in cell cycle progression. These observations suggest that p27 degradation by glucose limitation is cell cycle- and senescence-independent.

The energy-sensing LKB1-AMPK pathway is implicated in the induction of autophagy, resulting in cell survival under glucose-deprived conditions. Recently, Liang et al. showed that the LKB1-AMPK pathway regulates p27 phosphorylation at Thr198 and stabilizes p27 proteins.[52] They also indicated that accumulated p27 may play an important role in determining whether cells survive, become autophagic or undergo apoptosis under metabolic stress conditions.[52] Interestingly, neither the AMPK activator AICAR nor an AMPK inhibitor (compound C) affected p27 stability under glucose-deprived conditions (data not shown). However, we cannot exclude the possibility that

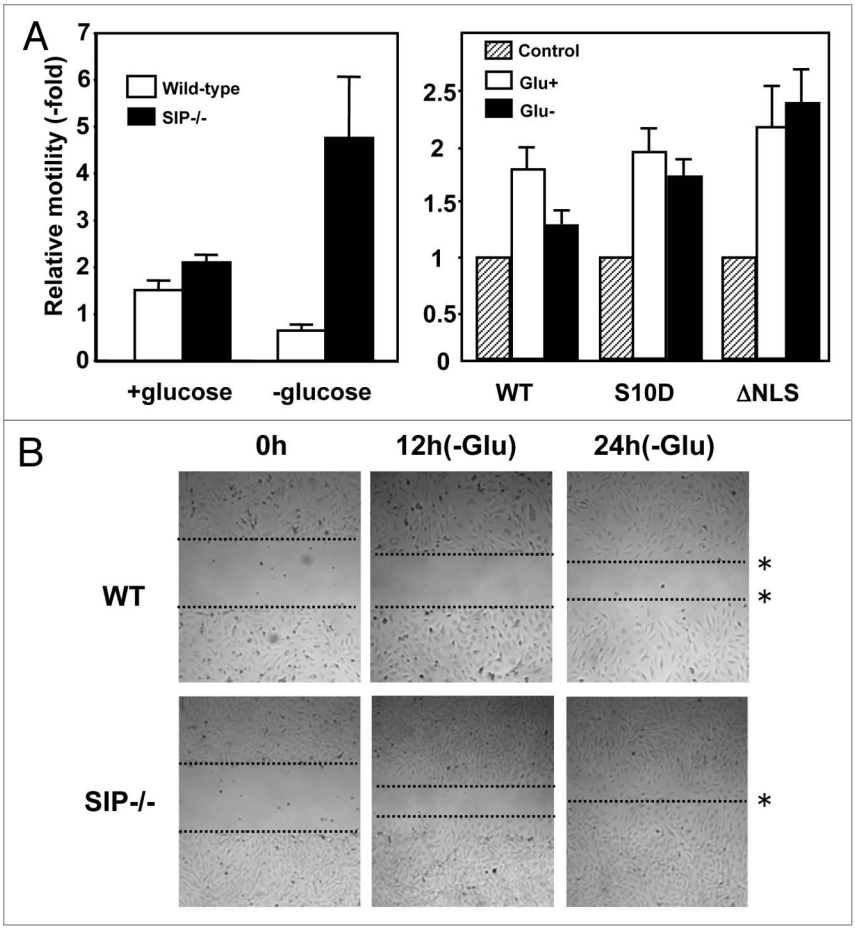

Figure 6. SIP regulates cell motility. (A) (Left) Serum-starved wild-type or *SIP*$^{-/-}$ MEFs were released into complete media or glucose-free media and allowed to migrate toward media containing 0.5% FBS or 10% FCS for 12 h. Colorimetric measurements were taken according to the manufacturer's instructions. (Right) 3T3 cells transfected with an empty pcDNA3 vector, pcDNA3 p27S10D or pc DNA3 p27ΔNLS were cultured in serum-starved media for 24 h, and were released into complete media or glucose-free media and allowed to migrate toward media containing 0.5% FBS or 10% FCS for 17 h. Colorimetric measurements were taken according to the manufacturer's instructions. (B) Serum-starved wild-type (WT) and *SIP*$^{-/-}$ MEFs were cultured in gelatin-coated 6-well plates to confluence and cells were introduced into media containing 2% FBS with (+Glu) or without glucose (-Glu). A wound area was mechanically induced by a single passage of a P200 tip across culture plate surface to confluent MEF monolayers. Cultures were continued for the indicated times and images obtained using light microscopy. Images were representative of six independent experiments. The dotted lines define the areas lacking cells.

Thr198 phosphorylation is indeed involved in the pathway where we detected p27 degradation.

How Siah1/SIP induces p27 degradation is enigmatic. It is also still unclear whether p27 binds to Siah1/SIP complex directly. The fact that phyl-peptide can inhibit the reaction suggests that the interaction requires an adaptor protein and is thus indirect. p27 is known to be degraded by the SCF^{Skp2} complex,[18-20] KPC1/2,[24] or Pirh2,[53] depending on which phase of the cell cycle is present. In particular, KPC1/2 contributes to the degradation of cytoplasmic p27 in the early G_1 phase.[24] Although our results indicate that glucose limitation-induced degradation of p27 is cell cycle-independent, we cannot neglect the possibility that the KPC complex might be involved in this degradation pathway. The F-box protein Skp2 acts as an adaptor that recognizes p27 phosphorylated on threonine residue 187 (T187) and facilitates p27 ubiquitination. In this regard, SIP is known to bind to the SCF-complex component Skp1, which provides a physical link between RING-finger proteins and the F-box proteins.[30] Our preliminary experiments suggest that overexpression of dominant-negative Skp2 or Ebi did not interfere Siah1-induced p27 degradation. These observations raise the possibility that an alternative F-box protein is involved in Siah1/SIP-mediated degradation of p27.

Though many studies suggested a role for p27 in cell migration, the physiological relevance of p27 stability controlled by glucose-deprived conditions has remained elusive. As shown here, glucose limitation suppresses motility of normal cells. Under such conditions, normal cells may rather differentiate than migrate, given that migration is an energy consuming process. Cell motility and migration play essential roles in many pathological processes such as metastasis, tumor angiogenesis and atherosclerosis,[54] and hypoglycemia may be connected to these disease states. For example, tumor cells are thought to be under conditions of hypoxia and hypoglycemia within the core of solid tumors prior to stimulation of angiogenesis. In this regard, the finding that many types of cancers contain high levels of cytosolic p27 raises the possibility that the Siah/SIP pathway for p27 degradation might be deregulated in cancer cells. Similarly, poorly controlled diabetes can result in intracellular glucose deficiency, because of insufficient insulin-induced glucose uptake. Thus, atherosclerosis might be accelerated in Siah/SIP-deficient diabetic animals. Thus, the role of Siah/SIP pathway for p27 degradation in the context of glucose dysregulation and disease warrants further evaluation.

Materials and Methods

Generation of SIP-deficient mice. SIP-deficient mice were generated as described previously in reference 39. All mice were maintained at animal facilities of the Sanford Burnham Medical Research Institute, according to institutional guidelines.

Plasmids. The cDNAs encoding various mutants or fragments of SIP, Siah1, Skp2 and β-Catenin were constructed as described previously in reference 30. The cDNA encoding the full length p27 were PCR-amplified from human placenta randomly-primed cDNA library. The mutants (S10D, ΔNLS) of p27 were generated by the site-directed mutagenesis method.[30]

Transfections, cell culture and cell cycle analysis. Culture and transient transfection of HEK293T and 3T3 cells was performed as described in reference 30. Primary MEFs were derived from E14.5 embryos according to standard protocols. Cells were cultured at 37°C (5% CO_2) in high-glucose Dulbecco's modified Eagle's medium (DMEM, Thermo Scientific) with 10% fetal calf serum (FCS), 1 mM L-glutamine containing penicillin and streptomycin (100 mg of each/L). For experiments using serum-starved cells, asynchronous cells at 70% confluence were washed with phosphate-buffered saline (PBS), and placed in DMEM containing 0.5% FCS for 48 h. For the time course experiments under glucose-deprived conditions, synchronized cells were washed with PBS, and placed in DMEM without glucose in the presence or absence of 10% FCS. Cell cycle analyses were performed as described in reference 39.

Immunoblotting and antibodies. Cells were lysed with RIPA buffer (50 mM TRIS-HCl (pH 7.4), 150 mM NaCl, 1% NP40, 0.1% SDS, 1 mM EDTA). To distinguish cytosolic and nuclear p27, cells were fractionated using Nuclear Extract Reagents (Active Motif) according to the supplier's manual. Briefly, cells were washed and harvested with PBS containing phosphatase inhibitor and the cells were resuspended in hypotonic buffer. Cell extracts were then centrifuged at 14,000x g for 30 sec, the cytosolic fraction collected and the nuclear pellets resuspended with complete lysis buffer. The cell extracts were then centrifuged at 14,000x g for 10 min to collect the nuclear fraction. Equal amounts of cell lysates were subjected to immunoblot analysis with antibodies to p27 (C-19, Santa Cruz), p-p27 Ser10 (Santa Cruz), Siah1 (N-15, Santa Cruz), CDK2 (M2, Santa Cruz), Hsc70 (K-19, Santa Cruz), α-tubulin (Zymed), Lamin-B1 (Zymed), LDH-A (N-14, Santa Cruz), c-Myc (9E10, Santa Cruz), HA (3F10, Roche) and FLAG (M2, Santa Cruz). Protein bands densitometry was performed using ImageJ software.

Immunoprecipitation assay. Cells (2 x 10^6) in 100 mm plates were used directly or transiently transfected with 3 μg (total) plasmid DNA. After 24 h, cells were treated with 1 μM MG132 for 6 h and lysed in 200 μl TNE solution containing 0.5% NP-40, 10 mM TRIS-HCl, pH 7.8, 0.15 M NaCl, 1 mM EDTA, 20 μM MG132 and protease inhibitor cocktail (complete, Mini, EDTA free, Roche). After preclearing with 20 μl protein G-Sepharose for 1 h at 4°C, immunoprecipitations were performed using 1 μg primary antibody (anti-p27 antibody; anti-Myc antibody) adsorbed to protein G-Sepharose beads at 4°C for 4 h. After washing in TNE solution, immune complexes were analyzed by SDS-PAGE/immunoblotting using various antibodies, including anti-Siah1 antibody (Abnova, 1–110) or anti-HA antibody or anti-ubiquitin antibody (FL-76, Santa Cruz and P4G7, Covance), followed by HRPase-conjugated anti-mouse or anti-rat immunoglobulin (GE health care UK limited) and detection using enhanced chemiluminescence (ECL) (West Pico, Thermo Scientific).

Ubiquitination assay. Myc-p27 (1.0 μg) and/or HA-ubiquitin (2.0 μg) and/or FLAG-tagged Siah1 (1.5 μg) were transfected into NIH3T3 cells. After 24 h, cells were treated with 1 μM MG132 for 6 h and harvested. Cell pellets lysed with RIPA buffer, containing 10 mM TRIS-HCl, pH 7.4, 1% NP40, 0.1% SDS, 0.15 M NaCl, 1 mM EDTA and protease inhibitor cocktail. Bead-bound proteins were then eluted in SDS sample buffer and subjected to immunoblot analysis with anti-HA antibody. The same membrane was stripped and reprobed with anti-Myc or FLAG polyclonal antibodies. For endogenous ubiquitination assay, MEFs were treated with 1 μM MG132 for 6 h before harvesting. Cells were lysed and immunoprecipitated with anti-p27 antibody. Each precipitate was divided into two parts, separated on SDS-PAGE and analyzed by immunoblotting with anti-ubiquitin and anti-p27 antibodies to detect ubiquitin-conjugated p27.

Cell migration assay. A transwell plate form cell migration assay kit (ECM508, Chemicon International) was used to check the cell motility. Briefly, cells were suspended in 0.3 ml culture medium with or without glucose, containing 0.1% FCS and were added to the upper chamber. Ten percent of FCS in the culture medium was plated in the lower chamber as a chemoattractant. Cells in the migration chambers were incubated in a humidified incubator for 24 h. The cells that traversed the membrane pore to the lower surface of the filter were stained with dye for visualization. The colorimetric measurement was performed at 560 nm.

In vitro wound healing assay. In vitro wound healing assays were performed for an additional method of following cell migration.[55,56] Serum-starved wild-type and *SIP*$^{-/-}$ MEFs were cultured in 6-well plates and released into complete media or glucose-free media. A wound area was mechanically induced by a single passage of a P200 tip across the culture plate surface to confluent MEF monolayers. Cells that migrated into the wounded area were visualized and photographed under an inverted microscopy.

Acknowledgments

We thank Y. Matsuzawa and J. Groos for technical assistance. This work was supported by the NIH (CA107403) and DoD W81XWH-05-1-0007.

Note

Supplemental materials can be found at:
www.landesbioscience.com/journals/cc/article/16912

References

1. Nourse J, Firpo E, Flanagan WM, Coats S, Polyak K, Lee MH, et al. Interleukin-2-mediated elimination of the p27^{Kip1} cyclin-dependent kinase inhibitor prevented by rapamycin. Nature 1994; 372:570-3; PMID: 7990932; DOI: 10.1038/372570a0.
2. Polyak K, Kato JY, Solomon MJ, Sherr CJ, Massague J, Roberts JM, et al. p27^{Kip1}, a cyclin-Cdk inhibitor, links transforming growth factor-beta and contact inhibition to cell cycle arrest. Genes Dev 1994; 8:9-22; PMID: 8288131; DOI: 10.1101/gad.8.1.9.
3. Toyoshima H, Hunter T. p27, a novel inhibitor of G_1 cyclin-Cdk protein kinase activity, is related to p21. Cell 1994; 78:67-74; PMID: 8033213; DOI: 10.1016/0092-8674(94)90573-8.
4. Coats S, Flanagan WM, Nourse J, Roberts JM. Requirement of p27^{Kip1} for restriction point control of the fibroblast cell cycle. Science 1996; 272:877-80; PMID: 8629023; DOI: 10.1126/science.272.5263.877.
5. Tsukiyama T, Ishida N, Shirane M, Minamishima YA, Hatakeyama S, Kitagawa M, et al. Downregulation of p27^{Kip1} expression is required for development and function of T cells. J Immunol 2001; 166:304-12; PMID: 11123306.
6. McAllister SS, Becker-Hapak M, Pintucci G, Pagano M, Dowdy SF. Novel p27^{kip1} C-terminal scatter domain mediates Rac-dependent cell migration independent of cell cycle arrest functions. Mol Cell Biol 2003; 23:216-28; PMID: 12482975; DOI: 10.1128/MCB.23.1.216-28.2003.

7. Besson A, Gurian-West M, Schmidt A, Hall A, Roberts JM. $p27^{Kip1}$ modulates cell migration through the regulation of RhoA activation. Genes Dev 2004; 18:862-76; PMID: 15078817; DOI: 10.1101/gad.1185504.
8. Fero ML, Rivkin M, Tasch M, Porter P, Carow CE, Firpo E, et al. A syndrome of multiorgan hyperplasia with features of gigantism, tumorigenesis and female sterility in $p27^{Kip1}$-deficient mice. Cell 1996; 85:733-44; PMID: 8646781; DOI: 10.1016/S0092-8674(00)81239-8.
9. Kiyokawa H, Kineman RD, Manova-Todorova KO, Soares VC, Hoffman ES, Ono M, et al. Enhanced growth of mice lacking the cyclin-dependent kinase inhibitor function of $p27^{Kip1}$. Cell 1996; 85:721-32; PMID: 8646780; DOI: 10.1016/S0092-8674(00)81238-6.
10. Nakayama K, Ishida N, Shirane M, Inomata A, Inoue T, Shishido N, et al. Mice lacking $p27^{Kip1}$ display increased body size, multiple organ hyperplasia, retinal dysplasia and pituitary tumors. Cell 1996; 85:707-20; PMID: 8646779; DOI: 10.1016/S0092-8674(00)81237-4.
11. Slingerland J, Pagano M. Regulation of the cdk inhibitor p27 and its deregulation in cancer. J Cell Physiol 2000; 183:10-7; PMID: 10699961; DOI: 10.1002/(SICI)1097-4652(200004)183:1<10::AID-JCP2>3.0.CO;2-I.
12. Philipp-Staheli J, Payne SR, Kemp CJ. $p27^{Kip1}$: regulation and function of a haploinsufficient tumor suppressor and its misregulation in cancer. Exp Cell Res 2001; 264:148-68; PMID: 11237531; DOI: 10.1006/excr.2000.5143.
13. Liang J, Zubovitz J, Petrocelli T, Kotchetkov R, Connor MK, Han K, et al. PKB/Akt phosphorylates p27, impairs nuclear import of p27 and opposes p27-mediated G_1 arrest. Nat Med 2002; 8:1153-60; PMID: 12244302; DOI: 10.1038/nm761.
14. Shin I, Yakes FM, Rojo F, Shin NY, Bakin AV, Baselga J, et al. PKB/Akt mediates cell cycle progression by phosphorylation of $p27^{Kip1}$ at threonine 157 and modulation of its cellular localization. Nat Med 2002; 8:1145-52; PMID: 12244301; DOI: 10.1038/nm759.
15. Viglietto G, Motti ML, Bruni P, Melillo RM, D'Alessio A, Califano D, et al. Cytoplasmic relocalization and inhibition of the cyclin-dependent kinase inhibitor $p27^{Kip1}$ by PKB/Akt-mediated phosphorylation in breast cancer. Nat Med 2002; 8:1136-44; PMID: 12244303; DOI: 10.1038/nm762.
16. Rosen DG, Yang G, Cai KQ, Bast RC Jr, Gershenson DM, Silva EG, et al. Subcellular localization of $p27^{kip1}$ expression predicts poor prognosis in human ovarian cancer. Clin Cancer Res 2005; 11:632-7; PMID: 15701850.
17. Denicourt C, Saenz CC, Datnow B, Cui XS, Dowdy SF. Relocalized $p27^{Kip1}$ tumor suppressor functions as a cytoplasmic metastatic oncogene in melanoma. Cancer Res 2007; 67:9238-43; PMID: 17909030; DOI: 10.1158/0008-5472.CAN-07-1375.
18. Carrano AC, Eytan E, Hershko A, Pagano M. SKP2 is required for ubiquitin-mediated degradation of the CDK inhibitor p27. Nat Cell Biol 1999; 1:193-9; PMID: 10559916; DOI: 10.1038/12013.
19. Montagnoli A, Fiore F, Eytan E, Carrano AC, Draetta GF, Hershko A, et al. Ubiquitination of p27 is regulated by Cdk-dependent phosphorylation and trimeric complex formation. Genes Dev 1999; 13:1181-9; PMID: 10323868; DOI: 10.1101/gad.13.9.1181.
20. Sutterlüty H, Chatelain E, Marti A, Wirbelauer C, Senften M, Muller U, et al. $p45^{SKP2}$ promotes $p27^{Kip1}$ degradation and induces S phase in quiescent cells. Nat Cell Biol 1999; 1:207-14; PMID: 10559918; DOI: 10.1038/12027.
21. Bashir T, Pagan JK, Busino L, Pagano M. Phosphorylation of Ser72 is dispensable for Skp2 assembly into an active SCF ubiquitin ligase and its subcellular localization. Cell Cycle 2010; 9:971-4; PMID: 20160477; DOI: 10.4161/cc.9.5.10914.
22. Woods TC. Regulation of cell migration by mTOR is mediated through changes in $p27^{Kip1}$ phosphorylation. Cell Cycle 2010; 9:2057-8; PMID: 20505330; DOI: 10.4161/cc.9.11.11927.
23. Malek NP, Sundberg H, McGrew S, Nakayama K, Kyriakides TR, Roberts JM. A mouse knock-in model exposes sequential proteolytic pathways that regulate $p27^{Kip1}$ in G_1 and S phase. Nature 2001; 413:323-7; PMID: 11565035; DOI: 10.1038/35095083.
24. Kamura T, Hara T, Matsumoto M, Ishida N, Okumura F, Hatakeyama S, et al. Cytoplasmic ubiquitin ligase KPC regulates proteolysis of $p27^{Kip1}$ at G_1 phase. Nat Cell Biol 2004; 6:1229-35; PMID: 15531880; DOI: 10.1038/ncb1194.
25. Kossatz U, Vervoorts J, Nickeleit I, Sundberg HA, Arthur JS, Manns MP, et al. C-terminal phosphorylation controls the stability and function of $p27^{kip1}$. EMBO J 2006; 25:5159-70; PMID: 17053782; DOI: 10.1038/sj.emboj.7601388.
26. Della NG, Senior PV, Bowtell DD. Isolation and characterisation of murine homologues of the Drosophila seven in absentia gene (sina). Development 1993; 117:1333-43; PMID: 8404535.
27. Hu G, Chung YL, Glover T, Valentine V, Look AT, Fearon ER. Characterization of human homologs of the Drosophila seven in absentia (sina) gene. Genomics 1997; 46:103-11; PMID: 9403064; DOI: 10.1006/geno.1997.4997.
28. Matsuzawa S, Takayama S, Froesch BA, Zapata JM, Reed JC. p53-inducible human homologue of Drosophila seven in absentia (Siah) inhibits cell growth: suppression by BAG-1. EMBO J 1998; 17:2736-47; PMID: 9582267; DOI: 10.1093/emboj/17.10.2736.
29. Reed JC, Ely K. Degrading Liaisons: Siah structure revealed. Nat Struct Biol 2002; 9:8-10; PMID: 11753426; DOI: 10.1038/nsb0102-8.
30. Matsuzawa SI, Reed JC. Siah-1, SIP and Ebi collaborate in a novel pathway for β-catenin degradation linked to p53 responses. Mol Cell 2001; 7:915-26; PMID: 11389839; DOI: 10.1016/S1097-2765(01)00242-8.
31. Filipek A, Kuznicki J. Molecular cloning and expression of a mouse brain cDNA encoding a novel protein target of calcyclin. J Neurochem 1998; 70:1793-8; PMID: 9572262; DOI: 10.1046/j.1471-4159.1998.70051793.x.
32. Filipek A, Jastrzebska B, Nowotny M, Kuznicki J. CacyBP/SIP, a calcyclin and Siah-1-interacting protein, binds EF-hand proteins of the S100 family. J Biol Chem 2002; 277:28848-52; PMID: 12042313; DOI: 10.1074/jbc.M203602200.
33. Matsuzawa S, Li C, Ni CZ, Takayama S, Reed JC, Ely KR. Structural analysis of Siah1 and its interactions with Siah-interacting protein (SIP). J Biol Chem 2003; 278:1837-40; PMID: 12421809; DOI: 10.1074/jbc.M210263200.
34. Santelli E, Leone M, Li C, Fukushima T, Preece NE, Olson AJ, et al. Structural analysis of Siah1-SIP interactions and insights into the assembly of an E3 ligase multiprotein complex. J Biol Chem 2005; 280:34278-87; PMID: 16085652; DOI: 10.1074/jbc.M506707200.
35. Amson RB, Nemani M, Roperch JP, Israeli D, Bougueleret L, Le Gall I, et al. Isolation of 10 differentially expressed cDNAs in p53-induced apoptosis: activation of the vertebrate homologue of the Drosphila seven in absentia gene. Proc Natl Acad Sci USA 1996; 93:3953-7; PMID: 8632996; DOI: 10.1073/pnas.93.9.3953.
36. Iwai A, Marusawa H, Matsuzawa S, Fukushima T, Hijikata M, Reed JC, et al. Siah-1L, a novel transcript variant belonging to the human Siah family of proteins, regulates beta-catenin activity in a p53-dependent manner. Oncogene 2004; 23:7593-600; PMID: 15326481; DOI: 10.1038/sj.onc.1208016.
37. Fiucci G, Beaucourt S, Duflaut D, Lespagnol A, Stumptner-Cuvelette P, Geant A, et al. Siah-1b is a direct transcriptional target of p53: identification of the functional p53 responsive element in the siah-1b promoter. Proc Natl Acad Sci USA 2004; 101:3510-5; Epub 2004 Feb 25.
38. Horikawa I, Fujita K, Harris CC. p53 governs telomere regulation feedback too, via TRF2. Aging (Albany NY) 2011; 3:26-32; PMID: 21266744.
39. Fukushima T, Zapata JM, Singha NC, Thomas M, Kress CL, Krajewska M, et al. Critical function for SIP, a ubiquitin E3 ligase component of the beta-catenin degradation pathway, for thymocyte development and G_1 checkpoint. Immunity 2006; 24:29-39; PMID: 16413921; DOI: 10.1016/j.immuni.2005.12.002.
40. House CM, Frew IJ, Huang HL, Wiche G, Traficante N, Nice E, et al. A binding motif for Siah ubiquitin ligase. Proc Natl Acad Sci USA 2003; 100:3101-6; PMID: 12626763; DOI: 10.1073/pnas.0534783100.
41. Bhatia B. On the move: $p27^{Kip1}$ drives cell motility in glioma cells. Cell Cycle 2010; 9:1231-40; PMID: 20404527; DOI: 10.4161/cc.9.7.11366.
42. See WL, Heinberg AR, Holland EC, Resh MD. p27 deficiency is associated with migration defects in PDGF-expressing gliomas in vivo. Cell Cycle 2010; 9:1562-7; PMID: 20404478; DOI: 10.4161/cc.9.8.11259.
43. Wu FY, Wang SE, Sanders ME, Shin I, Rojo F, Baselga J, et al. Reduction of cytosolic $p27^{Kip1}$ inhibits cancer cell motility, survival and tumorigenicity. Cancer Res 2006; 66:2162-72; PMID: 16489017; DOI: 10.1158/0008-5472.CAN-05-3304.
44. Yuan Y, Qin L, Liu D, Wu RC, Mussi P, Zhou S, et al. Genetic screening reveals an essential role of $p27^{kip1}$ in restriction of breast cancer progression. Cancer Res 2007; 67:8032-42; PMID: 17804714; DOI: 10.1158/0008-5472.CAN-07-0083.
45. Ishida N, Kitagawa M, Hatakeyama S, Nakayama K. Phosphorylation at serine 10, a major phosphorylation site of $p27^{Kip1}$, increases its protein stability. J Biol Chem 2000; 275:25146-54; PMID: 10831586; DOI: 10.1074/jbc.M001144200.
46. Rodier G, Montagnoli A, Di Marcotullio L, Coulombe P, Draetta GF, Pagano M, et al. p27 cytoplasmic localization is regulated by phosphorylation on Ser10 and is not a prerequisite for its proteolysis. EMBO J 2001; 20:6672-82; PMID: 11726503; DOI: 10.1093/emboj/20.23.6672.
47. Besson A, Assoian RK, Roberts JM. Regulation of the cytoskeleton: an oncogenic function for CDK inhibitors? Nat Rev Cancer 2004; 4:948-55; PMID: 15573116; DOI: 10.1038/nrc1501.
48. Ning X, Sun S, Hong L, Liang J, Liu L, Han S, et al. Calcyclin-binding protein inhibits proliferation, tumorigenicity and invasion of gastric cancer. Mol Cancer Res 2007; 5:1254-62; PMID: 18171983; DOI: 10.1158/1541-7786.MCR-06-0426.
49. Schneider G, Nieznanski K, Kilanczyk E, Bieganowski P, Kuznicki J, Filipek A. CacyBP/SIP interacts with tubulin in neuroblastoma NB2a cells and induces formation of globular tubulin assemblies. Biochim Biophys Acta 2007; 1773:1628-36.
50. Jones RG, Plas DR, Kubek S, Buzzai M, Mu J, Xu Y, et al. AMP-activated protein kinase induces a p53-dependent metabolic checkpoint. Mol Cell 2005; 18:283-93; PMID: 15866171; DOI: 10.1016/j.molcel.2005.03.027.
51. Carling D. The AMP-activated protein kinase cascade—a unifying system for energy control. Trends Biochem Sci 2004; 29:18-24; PMID: 14729328; DOI: 10.1016/j.tibs.2003.11.005.
52. Liang J, Shao SH, Xu ZX, Hennessy B, Ding Z, Larrea M, et al. The energy sensing LKB1-AMPK pathway regulates $p27^{kip1}$ phosphorylation mediating the decision to enter autophagy or apoptosis. Nat Cell Biol 2007; 9:218-24; PMID: 17237771; DOI: 10.1038/ncb1537.

53. Hattori T, Isobe T, Abe K, Kikuchi H, Kitagawa K, Oda T, et al. Pirh2 promotes ubiquitin-dependent degradation of the cyclin-dependent kinase inhibitor $p27^{Kip1}$. Cancer Res 2007; 67:10789-95; PMID: 18006823; DOI: 10.1158/0008-5472.CAN-07-2033.
54. Ridley AJ, Schwartz MA, Burridge K, Firtel RA, Ginsberg MH, Borisy G, et al. Cell migration: integrating signals from front to back. Science 2003; 302:1704-9; PMID: 14657486; DOI: 10.1126/science.1092053.
55. Khusial PR, Vadla B, Krishnan H, Ramlall TF, Shen Y, Ichikawa H, et al. Src activates Abl to augment Robo1 expression in order to promote tumor cell migration. Oncotarget 2010; 1:198-209; PMID: 21301049.
56. Wang L, Zhang J, Banerjee S, Barnes L, Sajja V, Liu Y, et al. Sumoylation of $vimentin_{354}$ is associated with PIAS3 inhibition of glioma cell migration. Oncotarget 2010; 1:620-7; PMID: 21317457.